

10
4-9-93 JSD

CONF 930269--10

SLAC-PUB--6067

DE93 010954

MODELLING RF SOURCES USING 2-D PIC CODES*

Kenneth R. Eppley

Stanford Linear Accelerator Center, Stanford University, Stanford, CA 94309 USA

ABSTRACT

In recent years, many types of RF sources have been successfully modelled using 2-D PIC codes. Both cross field devices (magnetrons, cross field amplifiers, etc.) and pencil beam devices (klystrons, gyrotrons, TWT's, lasertrons, etc.) have been simulated. All these devices involve the interaction of an electron beam with an RF circuit. For many applications, the RF structure may be approximated by an equivalent circuit, which appears in the simulation as a boundary condition on the electric field ("port approximation"). The drive term for the circuit is calculated from the energy transfer between beam and field in the drift space. For some applications it may be necessary to model the actual geometry of the structure, although this is more expensive. One problem not entirely solved is how to accurately model in 2-D the coupling to an external waveguide. Frequently this is approximated by a radial transmission line, but this sometimes yields incorrect results. We also discuss issues in modelling the cathode and injecting the beam into the PIC simulation.

INTRODUCTION

In recent years, 2-D PIC has been used to model a number of RF sources, e.g., klystrons, TWT's, lasertrons, magnetrons, CFA's, etc. We discuss a number of issues that arise in simulating RF devices, describe some successful solutions, and examine areas where difficulties still exist.

We separate the modelling process conceptually into several parts. The vacuum simulation involves the interior of the problem away from all boundaries. Beam injection requires modelling the cathode and transporting the beam into the interaction region. To model the RF structure one may either approximate the physical device with conducting boundaries, or else represent the circuit by imposing RF fields as a boundary condition to the vacuum region. Waveguides may also be modelled as RF boundary conditions, but they can present problems if the 3-D nature of the coupling invalidates the axisymmetric assumption. Surface physics must be understood to model secondary emission cathodes and multipactor.

VACUUM SIMULATION

Microwave tubes are well suited for PIC. The electron beams correspond to hot, low density plasmas, whose Debye length is of similar order to the scale of the RF structure. Although the internal temperature of the beams may be low,

* Work supported by the Department of Energy, contract DE-AC03-76SF00515.

MASTER

Invited talk presented at the Computational Accelerator Conference (CAP 93),
Pleasanton, CA, February 22-26, 1993

EB

the numerical heating rate is usually a function of the beam energy, which is high. The mesh size is generally determined by the RF structures rather than by the plasma properties. However, for relativistic beams, it may be necessary to reduce the mesh size to prevent unphysical emittance growth.

INJECTION

In pencil beam devices it is difficult to accurately simulate both the cathode region and the RF structure on a single mesh. Many Pierce guns have high convergence ratios. Thus the cathode radius is much larger than the drift tube. Also, the curved cathode surface cannot be modelled by stairsteps without grossly distorting the emission. For many guns, an electrostatic code such as EGUN gives an accurate calculation of the beam in the up to the RF region. Our klystron modelling uses EGUN, with a finer mesh and more radial trajectories than are used in the RF simulation, to generate a set of trajectories which are injected into the PIC simulation. Generally we reduce the number of radial trajectories by a factor of five to ten by averaging. It is important to properly model the space charge effects at the injection surface. Metal boundary conditions will cause a non-physical energy change. This is sometimes tolerable. However, for a long device it is often necessary to split the simulation into several pieces, injecting the output from one into the input of the next. In this situation a metal wall at the interface seriously distorts the bunching of the beam. We have found that using Neumann boundary conditions in the Poisson solver gives satisfactory results.

For an RF photocathode an electrostatic simulation would be inaccurate. When such devices have flat cathodes without radial compression, it is feasible to include the gun as part of the PIC calculation. One may model the actual electrode structure of the gun. Alternately, one may use EGUN to calculate the field distribution for the cathode region without space charge and impose this as a DC external field (either as a volume field or as a surface boundary condition).

RF STRUCTURE

One way of simulating an RF structure is to approximate the physical boundaries with conducting surfaces. Alternately, one may replace the structure with an equivalent circuit and impose its fields as a boundary condition on the simulation region. For a structure with a short fill time and simple boundaries, such as disks or vanes, modelling of the physical geometry is practical. This approach has been used in magnetrons and disk-loaded structures. For high-Q cavities, especially with reentrant noses, the second method, replacing the cavity gap by a voltage boundary condition ("port approximation") is highly useful. We describe this method in detail.

In the port approximation¹ to the modelling of RF cavities using an electromagnetic PIC code such as CONDOR², the cavities are simulated by imposing an RF voltage as a boundary condition across an opening or "port" in the outer wall

of the drift tube (Figure 1). This method ignores the transient and looks only for the steady-state solution at a single operating frequency. (This is done for speed, but if desired, the port method could be used to calculate the transient as well.) By writing the equations for energy flow across the gap, one splits the problem into two simpler pieces:

$$V \cdot I_{ind} = \int E \cdot J dV \quad (1)$$

(Dot product involves the integration over RF cycle of the complex phase; for vector quantities it also subsumes the spatial dot product.)

From the cavity side, in steady state the voltage across the gap and the current flowing in the walls uniquely determine the state of the cavity. From the drift tube side, the energy flow into or out of the beam is completely determined in steady state by the voltage and phase across the gap. The current flowing in the walls (the induced current) can be calculated simply in terms of the transform of the volume integral of $E \cdot J$. Of course, the current distribution is changed by the presence of the cavity voltage.

The voltage and phase must be chosen (by some means) to be consistent with the cavity impedance and with the RF current induced by the electron beam. Note that the induced current is not identical to the RF current flowing through the drift tube. The relation to cold cavity parameters comes through the relation

$$V = I_{ind}Z \quad (2)$$

It is straightforward to relate Z to cavity Q , ω , and R/Q (taking care to be consistent if voltages are measured on axis or across the gap), using the relationship:

$$Z = e^{j\psi}/\alpha \quad (3)$$

where

$$\alpha = I_{ind}/V = [Q_0^{-2} + 4(\Delta\omega/\omega)^2]^{1/2} \quad (4)$$

and

$$\psi = \phi_I - \phi_V = \tan^{-1}[-2Q_0\Delta\omega/\omega] \quad (5)$$

In steady state, the gap voltage should satisfy the condition

$$V_{ss} = I_{ss} \cdot Z \quad (6)$$

Here Z is the complex cavity impedance, and V_{ss} and I_{ss} are the Fourier components in steady state of the gap voltage and the induced current at the operating frequency. Now we assume a time dependence of the form:

$$V_t = V(t)e^{-j\omega t} \quad (7)$$

Here V_t is the instantaneous voltage across the port and $V(t)$ is an envelope which varies slowly in an RF cycle. Asymptotically, we want $V(t)$ to converge to V_{ss} . We can achieve this by making $V(t)$ satisfy a relaxation equation, i.e.,

$$dV(t)/dt = -k \cdot [V(t) - I(t) \cdot Z] \quad (8)$$

Thus $V(t)$ will adjust itself until the impedance relation is satisfied self-consistently. We compute the induced current at the operating frequency by keeping a running table of the volume integral of $E \cdot J$. The equation converges faster if one takes into account the beam loading, assuming that the change in induced current is a linear function of the change in voltage, i.e.

$$\Delta I = \alpha_l \cdot \Delta V \quad (9)$$

Then

$$\Delta V = -k\Delta t(V - IZ) \div (1 - \alpha_l Z) \quad (10)$$

The constant α_l depends on DC current, frequency, and drift-tube size but is insensitive to gap width and beam profile.

The port approximation has been used to calculate a number of klystrons at SLAC³ and has agreed with experiments to within about five percent in peak efficiency and to about two dB in gain (Figure 2).

An alternative to the port approximation is to model the cavity boundaries. This is feasible for low Q cavities or structures, but difficult for high Q gain cavities. An accurate gain calculation requires that the frequencies be correct to better than 0.1 percent. To avoid prohibitively fine zoning, it is necessary to "tweak" the cavity tuning by moving the boundaries a mesh point at a time. The MAGIC group has developed an algorithm so that their code can do this adjustment itself, rather than the user. This method works reasonably well, but

it does require an approximate knowledge of the cavity dimensions beforehand. It is slower than the port approximation, because it must run until the transient decays, and also because the simulation region is larger. As mentioned, the port method could be modified to compute the transient, if needed. The full cavity method is more accurate if the beam goes close to or intercepts the gap.

We have used full geometry modelling to simulate disk-loaded standing and travelling wave output structures (Figure 3). One can also use the port approximation to model some disk-loaded structures, using an impedance matrix to represent the coupling between the cells. This algorithm has been successful with slot-coupled standing wave double output cavities. If the inner radius of the disks is too large (e.g., if the drift tube is not cutoff to the second harmonic), the induced current calculation will be too inaccurate for the port approximation to be useable.

For narrow band structures, we have adopted the MAGIC idea of partially filling the outer mesh line for greater accuracy. We adjust the volume of metal to be the same as if the boundary were at its true physical location. Without this method, the mesh required for accurate resolution would be prohibitively fine. For disks with rounded ends on their inner radii such an adjustment would be more complex, and we have not yet attempted it.

Helical TWT's have been modelled using MAGIC⁴, representing the 3-D helix with an array of conducting wires and dielectric support rods (Figure 4). Although the simulation model was quite different geometrically from the physical helix, its RF properties were similar. The output was represented by a completely radiating freespace boundary. This model agreed well with experimental coldest results and hottest efficiency, except at low current.

Modelling the geometry in magnetrons is relatively simple, since the devices have low Q and the structures are usually vanes or slots. Periodicity allows one to model a single section with periodic boundary conditions. A full 360 degree simulation is sometimes necessary, if the output coupling is not periodic (Figure 5). There are also modes which only show up when the full circumference is included. CONDOR calculations of Varian phase-locked magnetrons⁵ agreed with experiment to about five percent in efficiency and to a few percent for the V-I characteristic (Figure 6).

Originally we believed that it was essential to use a capacitance matrix to properly impose the DC voltage on the anode. We have now found a simpler method to be satisfactory. We model the anode with conducting blocks and impose a voltage on the upper surface. Image charges on the conductors will force the field inside the metal to be zero.

Cross field amplifiers may be too long to model in their entirety. The RF sever makes this device non-periodic. We have used a variation on the port approximation to model such tubes. Rather than model each cell as a port, we

replaced the entire RF circuit with a traveling wave voltage imposed across the top boundary⁶. We again calculated the beam-circuit interaction from the energy balance equations. The simulation region corresponded to one travelling wave wavelength which moved with the electron spoke. In forward wave CFA's the power was quite variable, depending on how much bunching was maintained across the sever. Averaging over a number of passes gave reasonable agreement for a Varian CFA. The V-I curve agreed to about three percent and the efficiency to about fourteen percent.

COUPLING TO EXTERNAL WAVEGUIDES

In the port approximation, coupling to an output waveguide merely changes the Q of the cavity, with otherwise identical formalism. For the input waveguide, we make an initial calculation with a fixed voltage, independent of the specified drive level. We calculate the induced current on the input cavity and the voltages on the small signal cavities. Then we calculate the relation between input voltage and available power, and make a second calculation with the desired drive, scaling the small signal voltages linearly with the drive voltage.

For standing wave disk-loaded structures, coupling to a waveguide may be modelled by a port on the outer wall of the cell. The port behaves like a radial transmission line. We adjust the transmission coefficient of the port to produce the desired Q. Equivalently, we calculate the surface current from the magnetic field, then set the port voltage to equal $I \cdot Z$. We can vary Z to adjust the Q. If we need a complex impedance, we can Fourier transform the current to find the phase (for a single frequency). Another method, used in MAGIC, is to insert a resistive element behind the port and adjust the resistivity for a desired Q.

For a travelling wave structure the output coupling may be more complicated. Generally, these structures are adjusted experimentally to produce a good cold match. This adjustment may involve not only the waveguide geometry, but also the geometry of the cell previous to the waveguide. If we model the cells of a disk-loaded structure which was cold-matched in the lab, and adjust the impedance of the port (in general complex) for maximum transmission, then we get rough agreement between the 2-D model and the experimental device. Two such tubes built at SLAC agreed to ten percent in peak efficiency in such post-hoc simulations. We cannot always go the other way. A 2-D design that was fairly well matched in simulation was poorly matched in the lab. When the lab structure was adjusted to give a good match, its RF properties were very different from the originally simulated structure.

We are still studying this problem. We expect that if we could match the coldest voltages and phases in the simulation with coldest voltages and phases in the lab, then the hottest behavior would be similar. 3-D codes, which give good agreement with the lab, are still too slow to for extensive parameter studies. We

hope that by iterating between 2-D and 3-D calculations we will be able to obtain accurate answers in a reasonable timeframe.

For magnetrons we can also adjust the port impedance or transmission factor to get a desired Q. For a phase-locked magnetron, modelling the input cavity is somewhat more complex. This is because the input voltage does not remain constant in time, but will drop as a result of beam loading. Many simulations of magnetrons have ignored this effect. Including the beam loading effect, the voltage across the port is given by:

$$V_{port} = (1 + Z_-/Z_+) \cdot V_{input} - I_{wall} \cdot Z_- \quad (11)$$

where V_{input} is the incoming voltage on the waveguide, I_{wall} is the current flowing in the wall (calculated from the magnetic field), and Z_+ and Z_- are the forward and backward impedances of the waveguide. The relative sign of V and I is defined so that positive power corresponds to energy going into the tube. For a matched load, $Z_{load} = Z_+ = Z_-$, so $I = V_{port}/Z_{load}$, $V_{port} = V_{input}$, and there is no reflected wave.

SURFACE PHYSICS

Magnetrons and CFA's may use secondary emission to produce the electron beam. In CONDOR we used a universal curve with two parameters, peak yield and energy at the peak. We have used this model to simulate CFA's and magnetrons with platinum and oxide coatings. The oxide results generally agreed with a space charge limited current model, and to experimental data. At high current densities, the secondary emission model did not agree as well with the data as the space charge limited model. The secondary model predicted a peak current above which the current sheath was too depleted to replenish itself. Experimentally, higher currents were obtainable. The discrepancy might be due to the experimental coating having higher yields than assumed in the model, to 3-D variations in the spoke allowing the sheath to replenish itself, to a higher number of very low energy electrons being produced than were assumed in the model, or to some combination of these.

REFERENCES

1. K. Eppley, "Algorithms for the Self-Consistent Simulation of High Power Klystrons," *SLAC PUB 4622* (Stanford Linear Accelerator Center, May 1988).
2. B. Aiminetti, S. Brandon, K. Dyer, J. Moura, and D. Nielsen, Jr., *CONDOR User's Manual*, Livermore Computing Systems Document (Lawrence Livermore National Laboratory, Livermore, CA., April, 1988).
3. K. Eppley, A. Drobot, W. Herrmannsfeldt, H. Hanerfeld, D. Nielsen, S. Brandon, R. Malendez, "Results of Simulations of High Power Klystrons,"

Proceedings of the Particle Accelerator Conference (Vancouver, British Columbia, May, 1985).

4. B. Goplen, D. Smithe, K. Nguyen, M. Kodis, and N. Vanderplaats, "MAGIC Simulations and Experimental Measurements from the Emission Gated Amplifier Experiments," *Proceedings of the IEDM Meeting* (San Francisco, CA., December, 1992).
5. T. Treado, P. Brown, R. Bolton, T. Hansen, and K. Eppley, "High Power, High Energy, and High Efficiency Phase-Locked Magnetron Studies," *Proceedings of the IEDM Meeting* (Washington, D.C., December, 1991).
6. K. Eppley, "Numerical Simulation of Cross Field Amplifiers." *Proceedings of the Conference on Computer Codes and the Linear Accelerator Community* (Los Alamos, N.M., January, 1990).

Figure 1. Simulation of a real cavity by a port boundary condition.

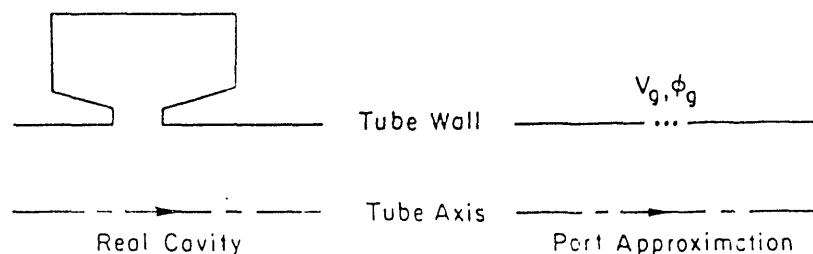


Figure 2. Comparison between CONDOR simulation and experimental results for the SLAC XC6 klystron.

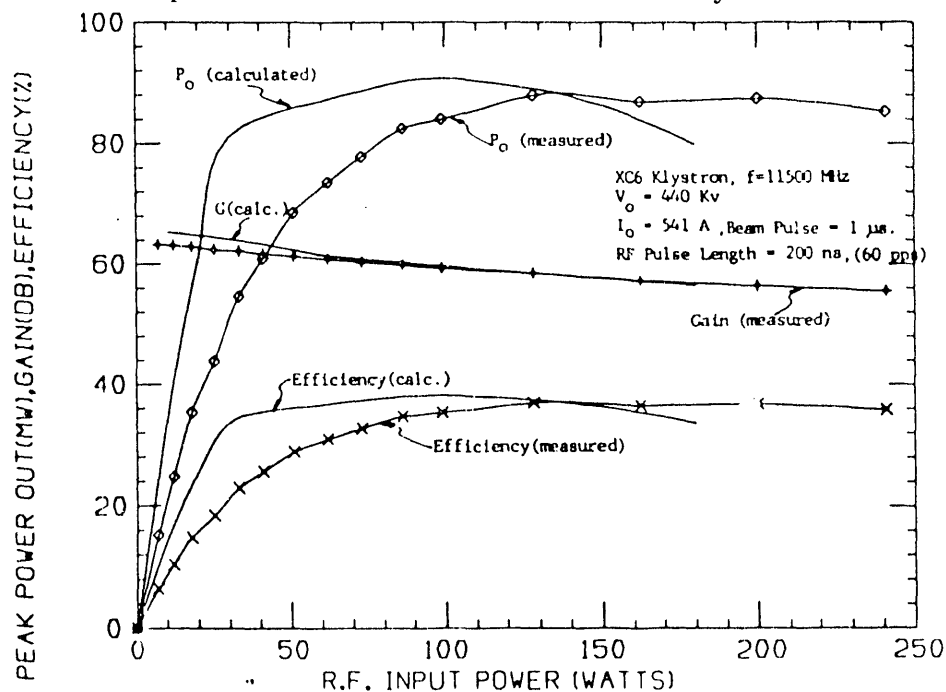


Figure 3. RF circuit and electron positions in a CONDOR simulation of an X-band disk-loaded output structure.

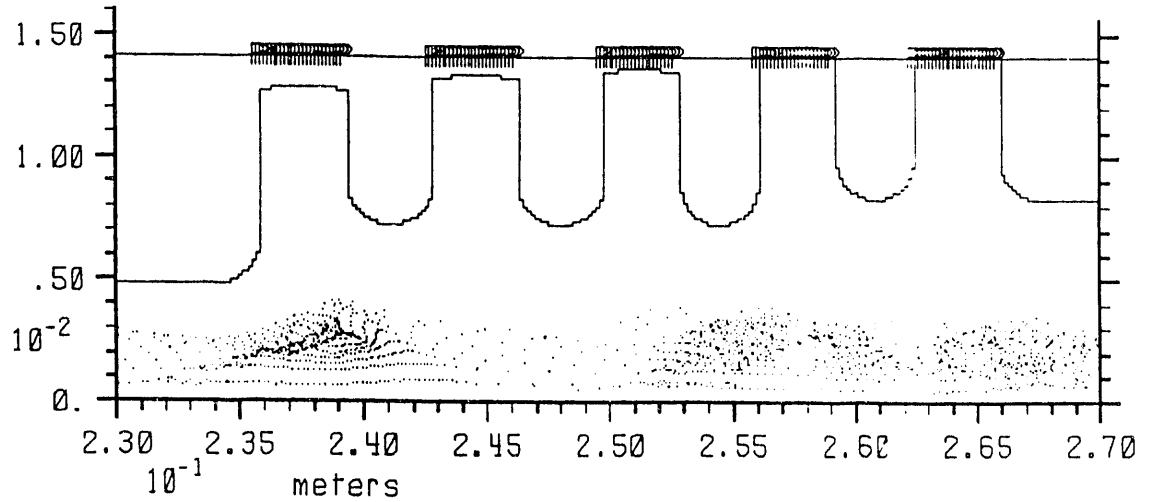


Figure 4. Simulation geometry used to model a helical travelling wave tube using MAGIC.

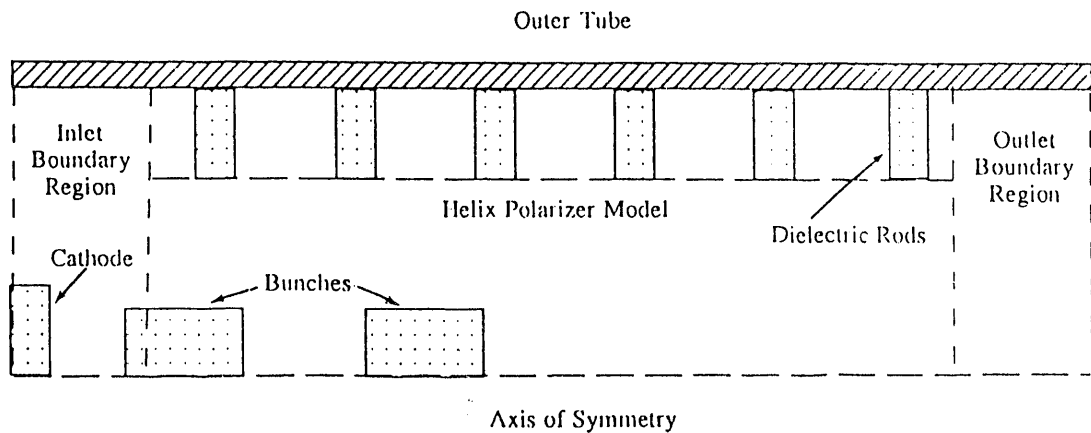


Figure 5. RF structure and electron distribution for a CONDOR simulation of a rising sun magnetron.

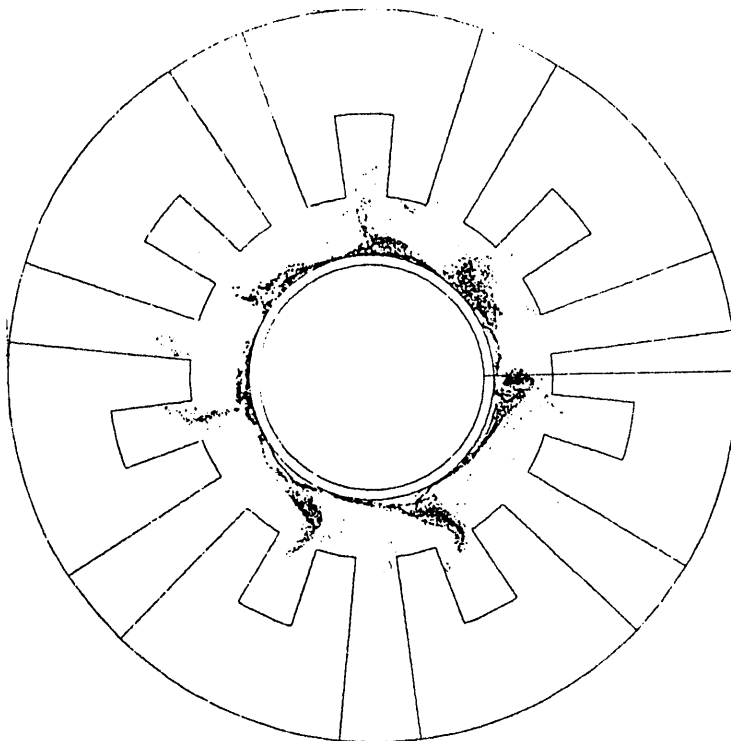
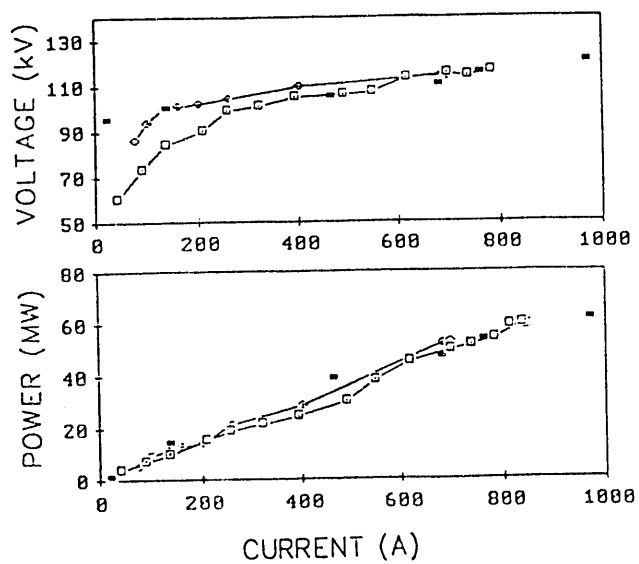


Figure 6. Comparison between simulation and experimental results for rising sun magnetrons. The open squares are experimental data. The closed squares are simulation results.



END

**DATE
FILMED**

6 / 22 / 93

